IOPscience iopscience.iop.org

Home Search Collections Journals About Contact us My IOPscience

Antiferromagnetism of RPtX (R = Ho, Er; X = Si, Ge) compounds

This article has been downloaded from IOPscience. Please scroll down to see the full text article.

1999 J. Phys.: Condens. Matter 11 5631

(http://iopscience.iop.org/0953-8984/11/29/310)

View the table of contents for this issue, or go to the journal homepage for more

Download details:
IP Address: 171.66.16.214
The article was downloaded on 15/05/2010 at 12:11

Please note that terms and conditions apply.

J. Phys.: Condens. Matter **11** (1999) 5631–5642. Printed in the UK PII: S0953-8984(99)00851-6

Antiferromagnetism of RPtX (R = Ho, Er; X = Si, Ge) compounds

B Penc†, S Baran†, M Hofmann‡, J Leciejewicz§, M Ślaski‖, A Szytuła†[+] and A Zygmunt¶

† Institute of Physics, Jagiellonian University, Reymonta 4, 30-059 Kraków, Poland
‡ Berlin Neutron Scattering Centre, Hahn-Meitner Institute, Berlin-Wannsee, Germany
§ Institute of Chemistry and Nuclear Technology, Warszawa, Poland
‖ School of Physics and Space Research, University of Birmingham, Edgbaston, Birmingham, UK
¶ W Trzebiatowski Institute of Low Temperature and Structural Research, Wrocław, Poland

E-mail: szytula@if.uj.edu.pl

Received 13 January 1999, in final form 17 March 1999

Abstract. X-ray and neutron diffraction as well as magnetometric measurements performed for HoPtX and ErPtX (X = Si, Ge) compounds indicate that they are crystalline and that they have the orthorhombic TiNiSi-type crystal structure. They are antiferromagnetic at low temperatures. A collinear magnetic structure with the propagation vector $\boldsymbol{k} = |1/2, 0, 1/2|$, stable between 1.5 K and the Néel point at 3.1 K is observed in HoPtSi. HoPtGe is paramagnetic at 1.8 K. A collinear magnetic order described by the wavevector $\boldsymbol{k}_1 = |0, 1/2, 0|$ has been found in ErPtSi and ErPtGe. As the temperature rises this structure transforms in both compounds into a sine modulated one with the wavevector $\boldsymbol{k}_2 = |0, k_y, 0|$. The Néel points of ErPtSi and ErPtGe are 4.0 and 4.1 K respectively.

1. Introduction

Ternary lanthanide compounds with the 1:1:1 stoichiometry containing transition metals T = *n*d ($n = 3, 4, 5$) and the p-electron elements X constitute today a large family of almost 1000 members [1]. They belong to over 30 different crystal structure types [2] and have been found to exhibit a variety of interesting magnetic and electrical properties [3]. To this family belong also RPtX compounds (R—lanthanide element, X = Si, Ge, Sn and Ga). A number of RPtSn stannides [4–7] and TbPtGa [8] were found to be antiferromagnetic at low temperatures, some of them undergo magnetic phase transitions. Therefore, as a part of our current research on magnetic properties of lanthanide ternaries with 1:1:1 stoichiometry, we have started neutron diffraction studies, supplemented by magnetometric and x-ray diffraction measurements on the lanthanide–platinum silicides and germanides.

In this paper we report the results obtained for HoPtSi, HoPtGe, ErPtSi and ErPtGe compounds. All of them show the orthorhombic TiNiSi type of crystal structure [9]. We expect that the obtained data will also contribute to the construction of the systematics of magnetic structures observed in TiNiSi-type phases.

[+] Corresponding author.

0953-8984/99/295631+12$30.00 © 1999 IOP Publishing Ltd

2. Experiment

RPtX samples (R = Ho, Er, X = Si, Ge) were synthesized by arc melting of stoichiometric amounts of high-purity constituent elements. The samples were subsequently annealed in vacuum for 100 h at 800 °C.

The samples were identified by their x-ray powder diagrams recorded using a Philips diffractometer (Co Kα radiation). All the x-ray reflections could be indexed in the orthorhombic TiNiSi type of crystal structure. The lattice parameters were determined and found to be in reasonable agreement with those reported earlier [4].

A SQUID magnetometer was used to measure the DC magnetization and magnetic susceptibility in the temperature range from 1.8 to 300 K. Additional magnetization data were obtained at $T = 4.2$ K on free powder samples oriented by the applied magnetic field using field strengths up to 120 kOe with the use of an Oxford Instruments VSM 12 T vibrating sample magnetometer. In the determination of the magnetization values no demagnetizing corrections have been made.

Neutron diffraction patterns were measured in the temperature range between 1.5 and 8 K using the E6 diffractometer at the BER II reactor in the Hahn–Meitner Institute in Berlin. Neutron patterns were not recorded for HoPtGe since the magnetometric data (see figure 1) revealed that this compound is paramagnetic still at 1.8 K. The neutron wavelength was 2.4383 Å. All data processing was done using the FULLPROF program [10] which defines also the R factor (table 1) as a criterion for the agreement between the neutron diffraction peak intensities observed and calculated for a particular model of the structure. The neutron scattering lengths were taken from [11] and the magnetic form factors for R^{3+} ions were adopted after [12]. The observed and calculated neutron intensities can be obtained on request from the corresponding author.

3. Results

3.1. Crystal structure

Neutron diffraction patterns, recorded in the paramagnetic state, confirmed that all the samples exhibit the orthorhombic crystal structure of the TiNiSi type with the $Pnma$ space group. The

Table 1. Crystal structure data for HoPtX and ErPtX (X = Si, Ge) compounds at $T = 8$ K.

Compound	HoPtSi	ErPtSi	ErPtGe
a (Å)	6.9158(14)	6.8917(73)	6.9105(48)
b (Å)	4.2482(23)	4.2445(39)	4.3266(28)
c (Å)	7.3791(44)	7.3982(75)	7.5296(60)
V (Å^3)	216.80(29)	216.41(65)	225.13(48)
x_R	−0.0102(102)	0.0087(65)	−0.0213(38)
z_R	0.6974(27)	0.7017(29)	0.7015(18)
x_{Pt}	0.2123(24)	0.1980(28)	0.2059(17)
z_{Pt}	0.0972(44)	0.1035(39)	0.0979(27)
x_x	0.3203(25)	0.3222(54)	0.3128(21)
z_x	0.4153(49)	0.4282(75)	0.4140(29)
R_{Bragg} (%)	10.9	12.0	7.16
R_{prof} (%)	10.2	10.2	8.04
$\sum x_i$	0.5326(49)	0.5202(82)	0.5187(38)
$\sum z_i$	0.5125(93)	0.5317(114)	0.5119(56)

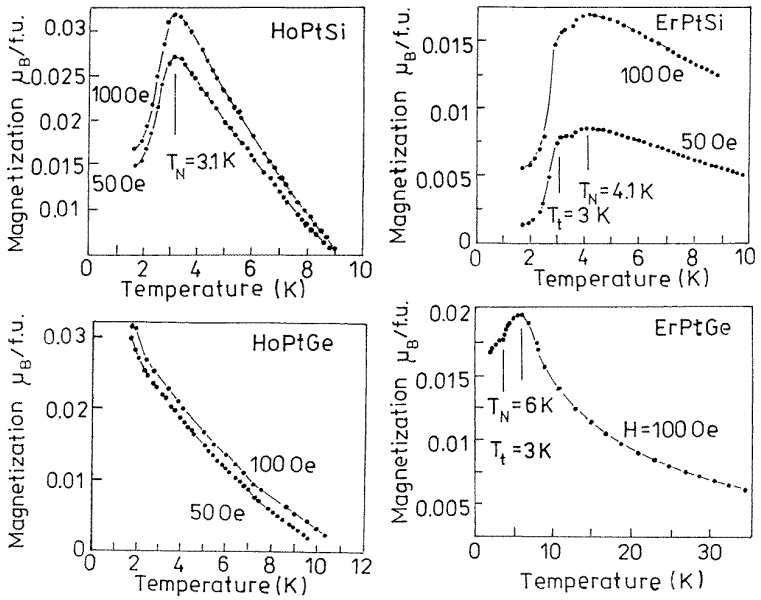

Figure 1. Temperature dependence of the magnetization of HoPtSi, ErPtSi, HoPtGe and ErPtGe.

Table 2. Magnetic data for HoPtX and ErPtX (X = Si, Ge) compounds.

								μ (μ_B)			
	T_N (K)		T_t (K)			μ_{eff} (μ_B)		Exp.			
Compound	M	ND	M	ND	θ_p (K)	Exp.	Theor.	[a]	[b]	Theor.	DMM
HoPtSi	3.1	3.1	—	—	−10.1	10.46	10.61	9.38(15)	9.7	10.0	$\parallel b$
HoPtGe	—	—	—	—	−6.7	10.32		—	8.7		
ErPtSi	4.1	4.0	3.0	2.5	−6.2	9.59	9.58	7.60(11)	7.6	9.0	$\parallel a$
ErPtGe	6.0	4.1	3.0	3.2	−11.5	9.50		7.79(8)	6.0		$\parallel a$

M—the values determined from the magnetic data.
ND—the values determined from the neutron diffraction data.
[a] the values of the rare earth magnetic moments in the ordered state determined from the neutron diffraction data at $T = 1.5$ K.
[b] the values of the magnetic moments determined from the magnetization measurements at $T = 4.2$ K and $H = 120$ kOe.
DMM—direction of the magnetic moment.

4(c) sites (x, 1/4, z; $\bar{x}$, 3/4, $\bar{z}$; 1/2 − x, 3/4, 1/2 + z; 1/2 + x, 1/4, 1/2 − z) are occupied by 4R, 4Pt and 4X (Si, Ge) atoms, each with different x and z parameters. The x and z values for the minimum of reliability factors R are listed in table 1.

3.2. Magnetic properties

Figure 1 displays the temperature dependence of the magnetization measured in magnetic fields of 50 and 100 Oe. The maxima indicating the onset of antiferromagnetic ordering are observed at 3.1 K for HoPtSi and 4.1 K for ErPtSi. In ErPtSi, below T_N an additional maximum in the

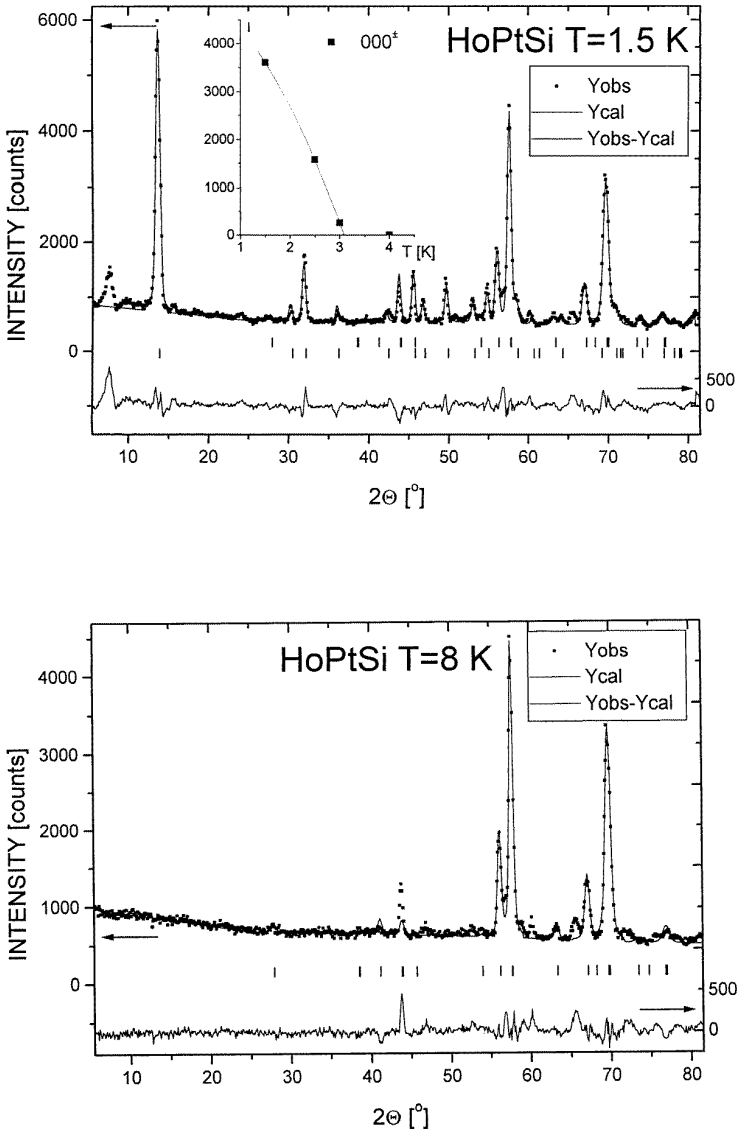

Figure 2. Observed and calculated neutron powder diffraction patterns of HoPtSi at 1.5 and 8 K. Open squares represent the observed points, solid lines are for the calculated profile and below a difference between the observed and calculated data is shown. Vertical bars indicate the molecular and magnetic peaks. The inset shows the temperature dependence of the $000^{\pm}$ reflections.

magnetization curve is observed at $T_t = 3$ K which is interpreted at the transition temperature between different magnetic phases. HoPtGe is paramagnetic down to 1.8 K. The temperature dependence of the magnetic susceptibility of ErPtGe gives a maximum corresponding to the Néel temperature at 6.0 K and additional maximum at $T_t = 3$ K.

For all the compounds the reciprocal magnetic susceptibility above the Néel temperature

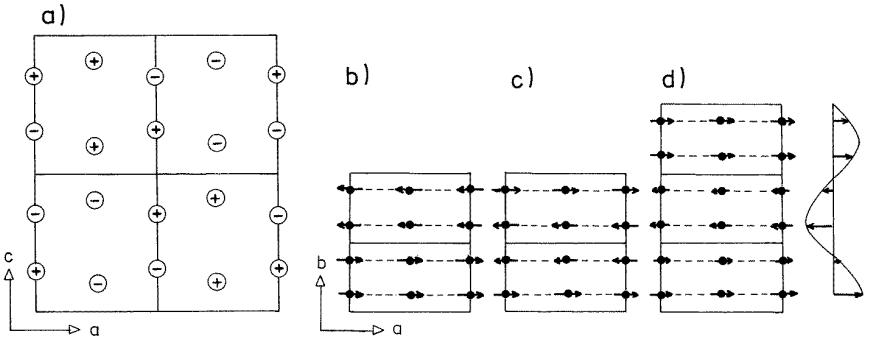

Figure 3. Projection of the magnetic structure of (a) HoPtSi on the *a*–*c*-plane and ErPtSi and ErPtGe on the *a*–*b*-plane for (b) F (ferromagnetic) mode, (c) G mode and (d) sine modulated structure.

obeys the Curie–Weiss law. The numerical fit to the experimental data yields the magnitudes of the effective magnetic moments μ_{eff} near the free R^{3+} ion values (see table 2). The paramagnetic Curie temperatures are negative and indicate that antiferromagnetic interactions are dominant in these compounds.

The magnetization curves at $T = 4.2$ K for all the compounds have paramagnetic character. The magnitudes of the magnetic moments at $T = 4.2$ K and $H = 120$ kOe are smaller than the free R^{3+} ion values (see table 2).

3.3. Magnetic structure

Neutron diffractograms recorded below the Néel temperatures for the investigated compounds reveal the presence of additional peaks of magnetic ordering.

The lanthanide magnetic moments occupy the following positions in the crystal unit cell:

$\boldsymbol{S}_1(x, 1/4, z)$; $\boldsymbol{S}_2(\bar{x}, 3/4, \bar{z})$; $\boldsymbol{S}_3(1/2 - x, 3/4, 1/2 + z)$ and $\boldsymbol{S}_4(1/2 + x, 1/4, 1/2 - z)$.

The Bertaut theory [13] constructed on the basis of an irreducible representation for spin transformation of the 4(c) site in the space group $Pnma$ gives one ferro-: $\boldsymbol{F} = \boldsymbol{S}_1 + \boldsymbol{S}_2 + \boldsymbol{S}_3 + \boldsymbol{S}_4$ and three antiferromagnetic structures described by the vectors:

$$\boldsymbol{G} = \boldsymbol{S}_1 - \boldsymbol{S}_2 + \boldsymbol{S}_3 - \boldsymbol{S}_4 \qquad \boldsymbol{C} = \boldsymbol{S}_1 + \boldsymbol{S}_2 - \boldsymbol{S}_3 - \boldsymbol{S}_4 \qquad \boldsymbol{A} = \boldsymbol{S}_1 - \boldsymbol{S}_2 - \boldsymbol{S}_3 + \boldsymbol{S}_4.$$

3.3.1. HoPtSi. The neutron diffraction pattern of HoPtSi recorded at $T = 1.5$ K shows additional peaks which are indexed with the wavevector $\boldsymbol{k} = (1/2, 0, 1/2)$ (figure 2). The distribution of the peaks is similar to that observed in the isostructural HoRhSi [14, 15], HoNiSi [16], HoNiGe [17] and HoRhGe [18]. The Ho magnetic moment equal to 9.38(15) μ_B forms a collinear magnetic structure described by the $\boldsymbol{C}$-vector with the moment parallel to the *b*-axis. The reliability factor (R) between the observed and calculated magnetic intensities is 11.8%. The projection of this structure on the *a*–*c*-plane is shown in figure 3(a). The temperature dependence of the magnetic intensity of the $000^{\pm}$ reflection gives the Néel temperature at 3.1 K.

3.3.2. ErPtSi and ErPtGe. The magnetic peaks observed in the neutron diffraction patterns of ErPtSi and ErPtGe at $T = 1.5$ K are indexed with the wavevector $\boldsymbol{k}_1 = (0, 1/2, 0)$ (see

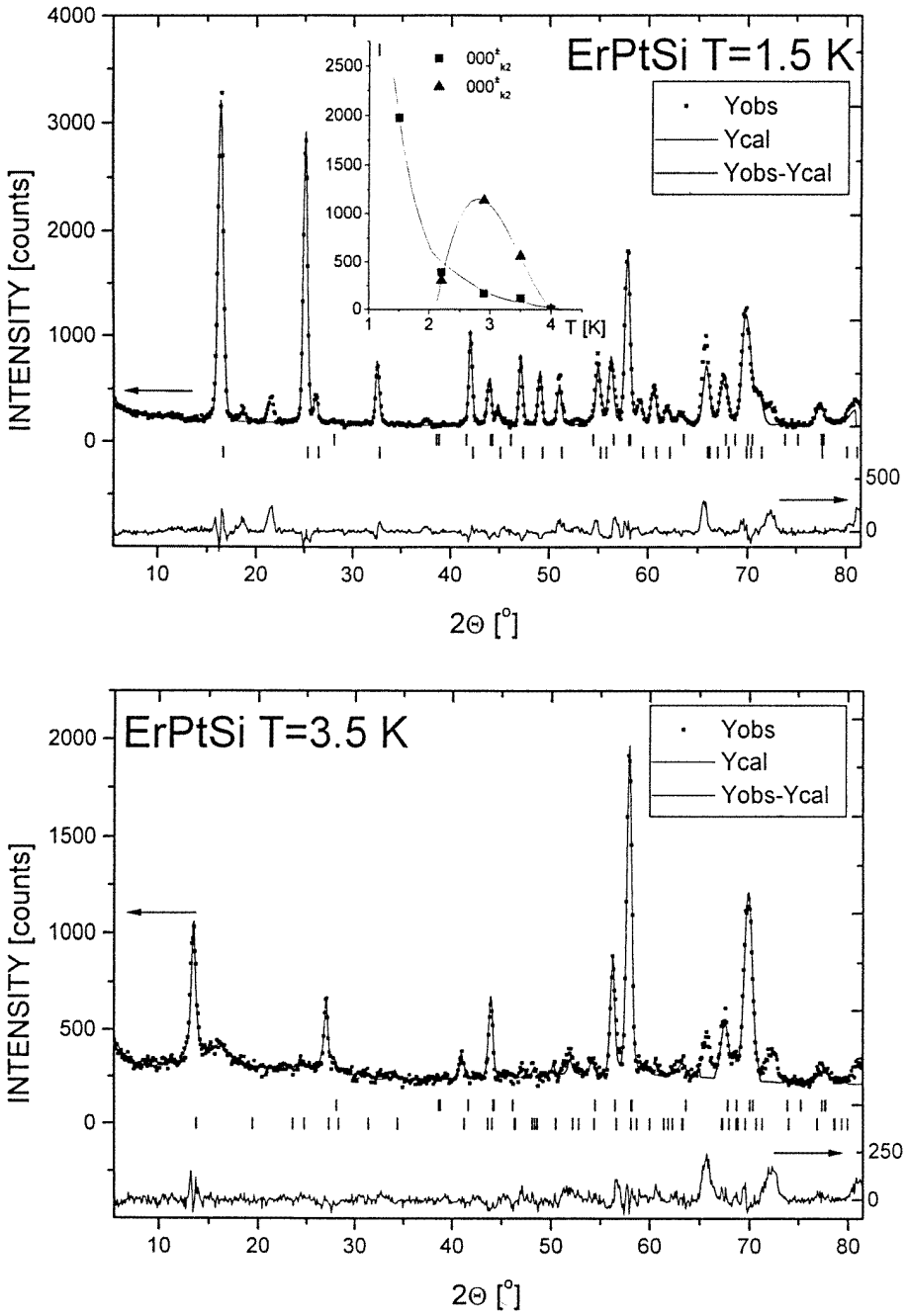

Figure 4. Observed and calculated neutron diffraction patterns of ErPtSi at $T = 1.5$, 3.5 and 8 K. Open squares represent the observed points, solid lines are for the calculated profile and below a difference between the observed and calculated data is shown. Vertical bars indicate the molecular and magnetic peaks. The inset shows the temperature dependence of the $000^{\pm}$ reflections corresponding to the commensurate and incommensurate phases.

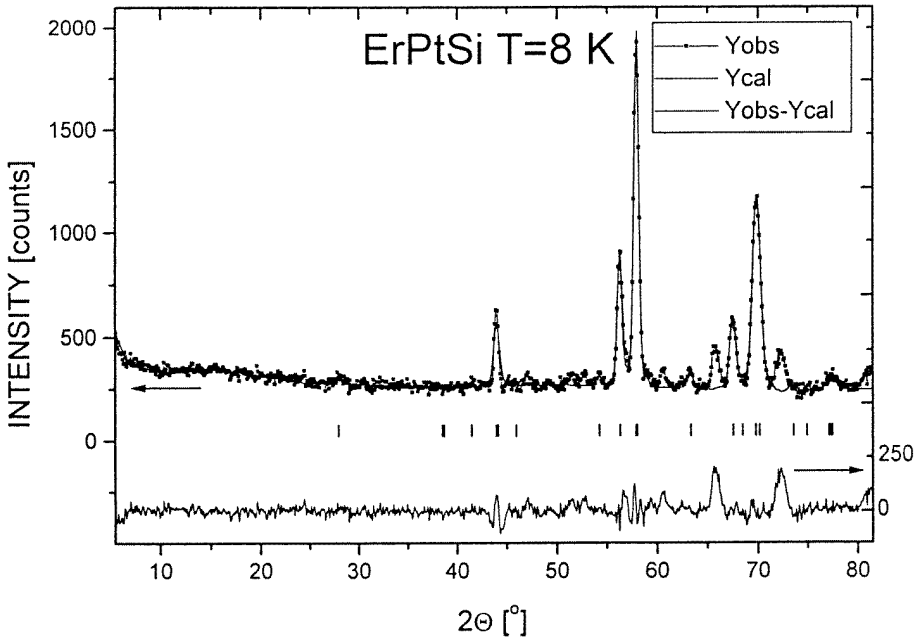

Figure 4. (Continued)

figures 4 and 5). The magnetic unit cell is doubled along the b-axis with respect to the crystallographic cell. Two models of moment distribution could be constructed, each giving almost the same value of the conventional reliability factor R. The latter indicates the fit of the neutron magnetic intensities calculated for a given model to the observed ones. In the first model, the Er^{3+} magnetic moments are coupled ferromagnetically (F mode) inside the crystallographic cell, but antiferromagnetically in the magnetic cell (see figure 3(b)). For this structure the R-factors are: 10.6% (ErPtSi) and 7.34% (ErPtGe). In the alternative model the Er^{3+} moments are coupled $+ - +-$ (G mode) inside the crystallographic unit cell and antiferromagnetically in the magnetic cell (figure 3(c)). The latter model gives the same R-factors for both compounds and the Er^{3+} moments aligned along the a-axis. At 1.5 K the moment amounts to 7.60(11) μ_B and 7.79(8) μ_B in ErPtSi and ErPtGe, respectively.

With increase of the temperature a change of the positions of the magnetic peaks is observed at $T_t = 2.5$ K for ErPtSi and $T_t = 3.2$ K for ErPtGe. The positions of these peaks are indexed with the wavevector $\boldsymbol{k}_2 = (0, k_y, 0)$, where $k_y = 0.416(1)$ for ErPtSi and 0.406(1) for ErPtGe at $T = 3.5$ K. The Er magnetic moments are parallel to the a-axis. The reliability factors R are 9.7% for ErPtSi and 11.5% for ErPtGe. The temperature dependence of the magnetic intensities gives the Néel temperature 3.8 K for ErPtSi and at 4.1 K for ErPtGe.

4. Discussion

The neutron diffraction data confirmed that HoPtSi, ErPtSi and ErPtGe compounds crystallize in the orthorhombic TiNiSi type of crystal structure. The determined atomic parameters for Pt and X = Si, Ge fulfill the following relation: the sum values $\sum x_i$ of the x-coordinates of Pt and

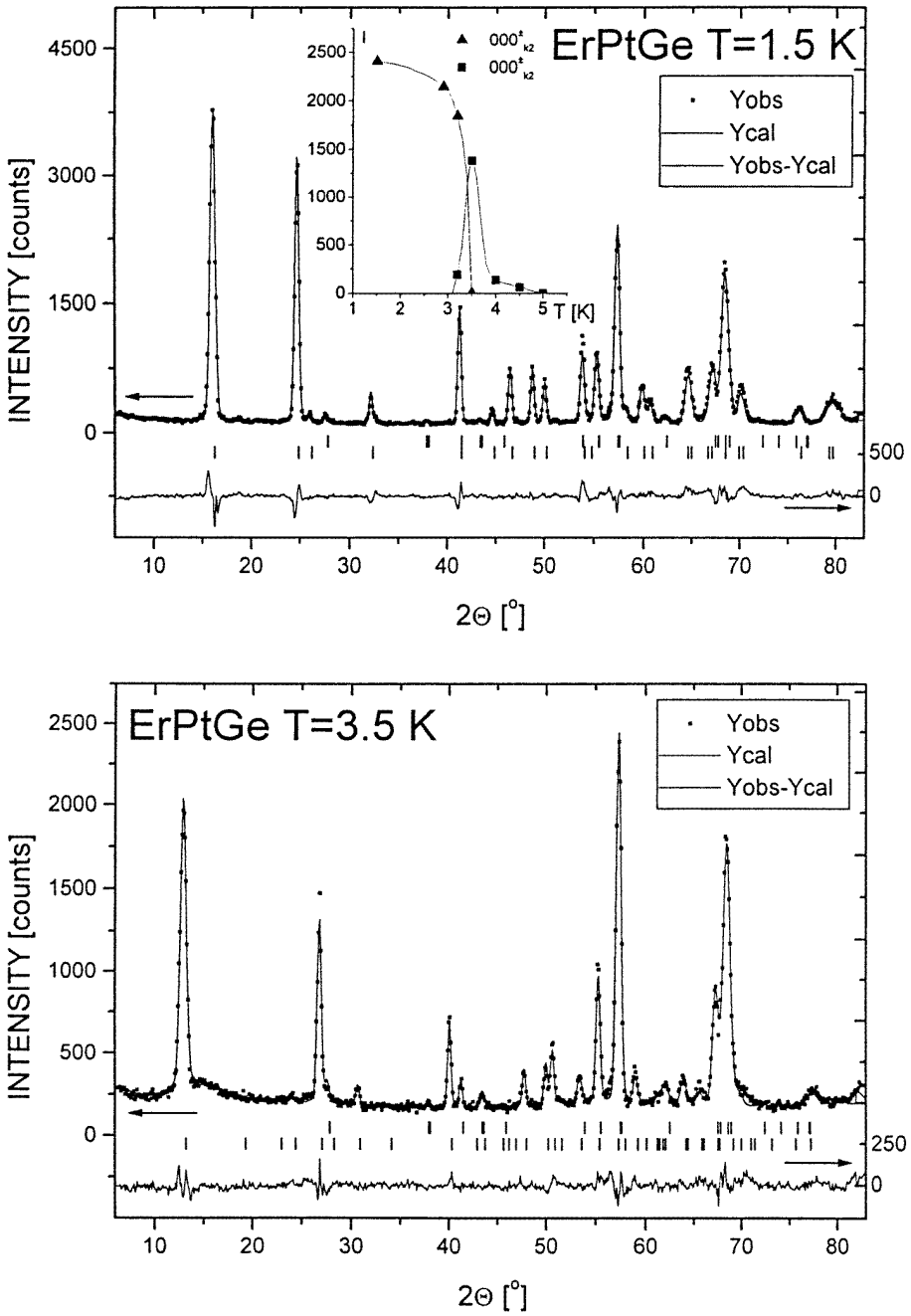

Figure 5. Observed and calculated neutron diffraction patterns of ErPtGe recorded at 1.5, 3.5 and 8 K. Open squares represent the observed points, solid lines are for the calculated profile and below a difference between the observed and calculated data is shown. Vertical bars indicate the molecular and magnetic peaks. The inset shows the temperature dependence of the $000^{\pm}$ reflections corresponding to the commensurate and incommensurate phases.

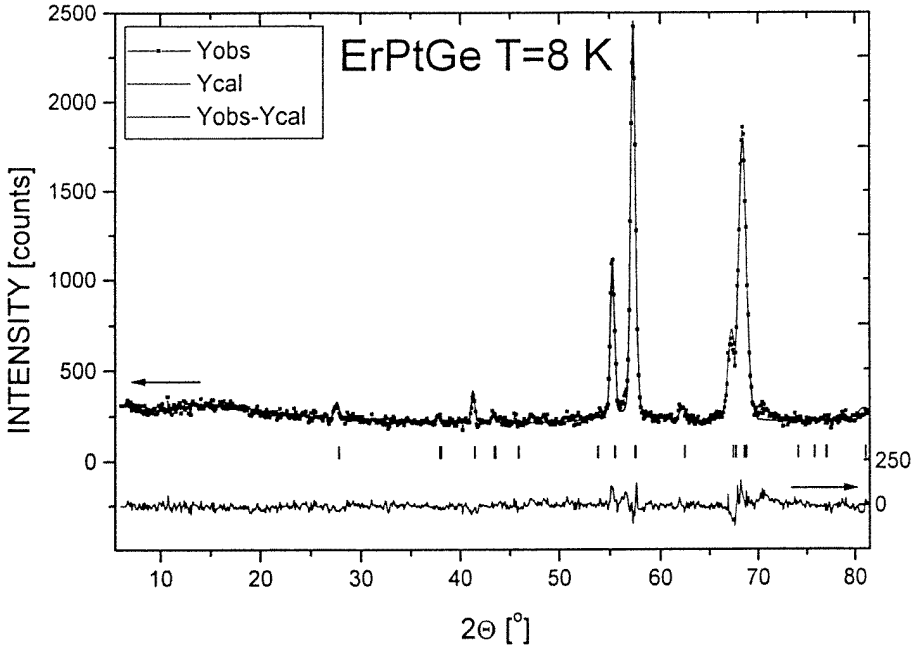

Figure 5. (Continued)

X elements is almost the same as the sum values $\sum z_i$ of the corresponding z-coordinates and is close to $1/2$ (see table 1). All component atoms of these compounds occupy four available 4(c) sites, each characterized by a mirror plane $b = 1/4$. Figure 6 shows the distribution of all atoms in the crystal unit cell. The rare earth atoms form wavy chains running along the a-axis with large R–R separation (e.g. 3.54 Å in HoPtSi). The chains form mirror planes normal to the b-axis with intersection parameter $y = 1/4$ and $3/4$. The antiphase relative position of rare earth chains of the adjacent planes creates two values of R–R distances between their atoms. For HoPtSi they are equal to 3.60 Å and 4.95 Å.

The data presented in this work indicate that the magnetic moment is localized only on the lanthanide atom. The observed interatomic distances between these atoms suggest that direct magnetic interactions are highly improbable. The stability of the observed magnetic ordering scheme may thus be considered as due to the interactions via conduction electrons (RKKY model).

The magnetic structure of HoPtSi is similar to that observed in the isostructural silicides (HoRhSi [14, 15], HoNiSi [16]) and germanides (HoNiGe [17], HoRhGe [18]). In all these compounds the holmium magnetic moments at $T = 1.5$ K form a collinear magnetic structure with the magnetic unit cell doubled along the a- and c-axis with respect to the crystallographic cell. In all these compounds magnetic moments are parallel to the b-axis. In the compounds with Rh the magnetic structure remains stable up to the Néel temperature. A different situation is observed in Ni compounds: near the Néel temperature a change to a modulated structure is observed. HoPtGe similarly to HoIrGe [19] is paramagnetic down to 1.5 K. HoRuGe forms a non-collinear ferromagnetic structure [20].

At low temperatures ErPtSi and ErPtGe exhibit a collinear antiferromagnetic structure with

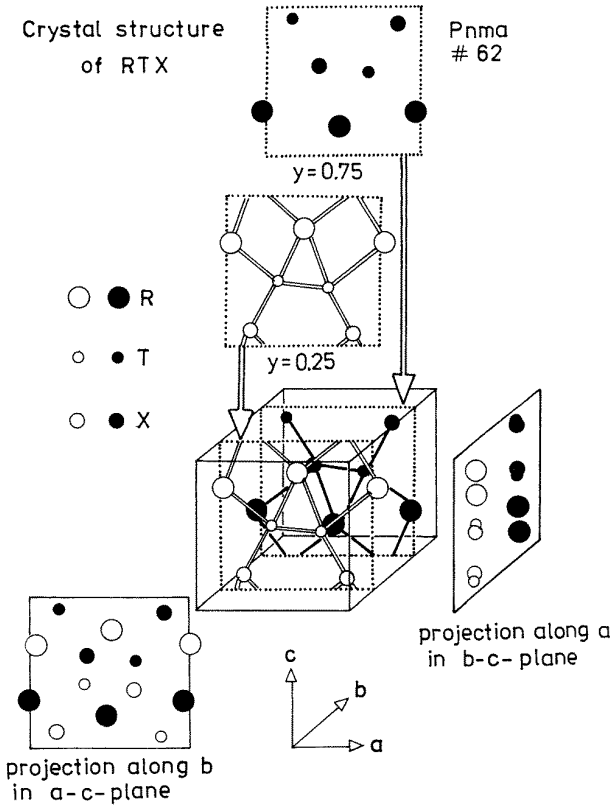

Figure 6. Crystal structure of RTX compounds and its projections on the *a*–*c*- and *b*–*c*-planes.

the magnetic unit cell doubled along the *b*-axis in respect to the crystallographic cell. As the temperature rises, a change to the sine modulated structure with the wave vector $\boldsymbol{k} = (0, k_y, 0)$ is observed. A similar temperature dependence of the magnetic structure has been found in other isostructural compounds.

The Néel temperatures as a function of the atomic volume V for the discussed compounds are presented in figure 7. The observed oscillatory dependence of the Néel temperature is in agreement with the sinusoidal character of the formula for the exchange integral postulated by the RKKY model [21–23]. The maxima of T_N observed in figure 7 for different values of V are due to different R–R distances in the silicides and germanides.

The second factor which influences the magnetic ordering is the crystalline electric field (CEF). In the CEF Hamiltonian related to the C_s symmetry in the TiNiSi type of crystal structure the second order CEF parameter B_2^0 is dominant. Its magnitude and sign determine the direction of the magnetic moment. The experimental data [24] and the results of the point charge calculation of the crystal field parameters for the isostructural RSi compounds [25] indicate that for a negative sign of the B_2^0 parameter the magnetic moment is parallel to the *b*-axis, whereas for a positive sign the moment lies in the *a*–*c*-plane. For HoTX compounds the magnetic moments are parallel to the *b*-axis, while for ErTX compounds they are parallel to the *a*-axis. This result indicates the change of the sign of the B_2^0 parameter from negative for

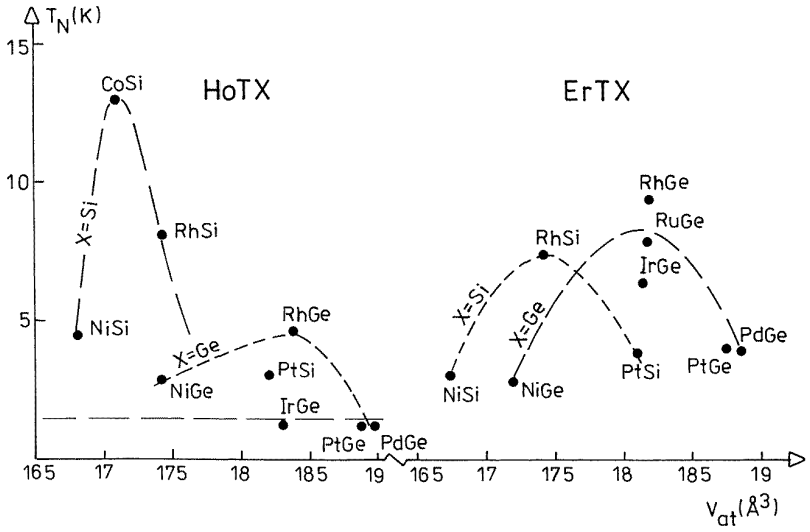

Figure 7. Néel temperatures of HoTX and ErTX compounds plotted against the atomic volume. The horizontal dashed line indicates the 1.5 K temperature limit of the experiments.

Ho compounds to positive for Er compounds. A similar effect was reported for many RT_2X_2 compound with the tetragonal $ThCr_2Si_2$ type of structure [26].

A change of the magnetic structure from a commensurate one at low temperatures to an incommensurate one near the Néel temperature observed in HoNiX and ErPtX compounds has been explained in terms of a realistic mean field model which takes into account the temperature changes of the periodic field and the crystal electric field [27].

Acknowledgments

The kind hospitality and financial support by the Hahn–Meitner Institute to perform neutron experiments is gratefully acknowledged by four of the authors (SB, JL, BP and AS). This work has been supported in part by the State Committee for Scientific Research in Poland with grant No 270/P03/98/15.

References

[1] Villars P and Calvert L D 1991 *Pearsons Handbook of Crystallographic Data for Intermetallic Phases* 2nd edn (Materials Park, OH: ASM International)
[2] Fornasini M L and Merlo F 1995 *J. Alloys Compounds* **219** 63
[3] Szytuła A and Leciejewicz J 1994 *Handbook of Crystal Structures and Magnetic Properties of Rare Earth Intermetallics* (Boca Raton, FL: Chemical Rubber Company)
[4] Kolenda M, Leciejewicz J, Stüsser N, Szytuła A and Zygmunt A 1995 *J. Magn. Magn. Mater.* **145** 85
[5] Szytuła A, Penc B, Kolenda M, Leciejewicz J, Stüsser N and Zygmunt A 1996 *J. Magn. Magn. Mater.* **153** 273
[6] Szytuła A, Kolenda M, Leciejewicz J and Stüsser N 1996 *J. Magn. Magn. Mater.* **164** 377
[7] Kadowaki H, Ekimo T, Iwasaki H, Takbotake T, Fujii H and Sakurai J 1993 *J. Phys. Soc. Japan* **62** 4426
[8] Schäfer W, Jansen E, Will G, Kotsanidis P A, Yakinthos J K and Tietza-Jaensch E 1994 *J. Alloys Compounds* **206** 225
[9] Hovestreydt E, Engel N, Klepp K, Chabot B and Parthé E 1982 *J. Less. Common. Met.* **85** 247

[10] Rodriguez-Carvajal J 1993 *Physica* B **192** 55
[11] Sears V F 1992 *Neutron News* **3** 26
[12] Freeman A J and Deslaux J P 1979 *J. Magn. Magn. Mater.* **12** 11
[13] Bertaut E F 1968 *Acta Crystallogr.* A **24** 217
[14] Bażela W, Leciejewicz J and Szytuła A 1985 *J. Magn. Magn. Mater.* **50** 19
[15] Quezel S, Rossat-Mignod J, Chevalier B, Wang Xian Zhong and Etourneau J 1985 *C. R. Acad. Sci. Paris* II **301** 919
[16] Szytuła A, Bałanda M, Hofmann M, Leciejewicz J, Kolenda M, Penc B and Zygmunt A 1999 *J. Magn. Magn. Mater.* **191** 122
[17] André G, Bourée F, Bombik A, Oleś A, Sikora W, Kolenda M and Szytuła A 1993 *J. Magn. Magn. Mater.* **127** 83
[18] Bażela W, Hofmann M, Penc B and Szytuła A 1998 *J. Phys.: Condens. Matter* **10** 2233
[19] Penc B, Hofmann M, Leciejewicz J, Ślaski M and Szytuła A 1999 *J. Alloys Compounds* at press
[20] Penc B, Hofmann M and Szytuła A 1999 *J. Alloys Compounds* at press
[21] Cogblin B 1977 *The Electronic Structure of Rare Earth Metals and Alloys: the Magnetic Heavy Rare Earth* (London: Academic)
[22] Rocher Y A 1963 *Adv. Phys.* **11** 233
[23] Mattis D C 1965 *The Theory of Magnetism* (New York: Harper and Row) p 195
[24] Kurisu M, Hori H, Furusawa M, Miyake M, Andoh Y, Oguro I, Kindo K, Takeuchi T and Yamagisho A 1994 *Physica* B **201** 107
[25] Nguyen V N, Rossat-Mignod J and Tchéou F 1975 *Phys. Status Solidi* a **17** 101
[26] Szytuła A and Leciejewicz J 1989 *Handbook on the Physics and Chemistry of Rare Earths* vol 12, ed K A Gschneidner and L Eyring (Amsterdam: North-Holland) p 133
[27] Gignoux D and Schmitt D 1993 *Phys. Rev.* B **84** 12 682